PB90-219759

Compact Coiled Denuder for Atmospheric Sampling

MSP Corp., Minneapolis, MN

Prepared for:
Environmental Protection Agency, Research Triangle Park, NC

1990

U.S. Department of Commerce
National Technical Information Service
NTIS

TECHNICAL REPORT DATA
(Please read Instructions on the reverse before complet

1. REPORT NO.	2.	3.
EPA/600/J-90/030		PB90-219759

4. TITLE AND SUBTITLE	5. REPORT DATE
A COMPACT COILED DENUDER FOR ATMOSPHERIC SAMPLING	6. PERFORMING ORGANIZATION CODE
7. AUTHOR(S) D.Y.H. Pui, C.-J. Tsai, B.Y.H. Liu (and C.W. Lewis AREAL)	8. PERFORMING ORGANIZATION REPORT NO.
9. PERFORMING ORGANIZATION NAME AND ADDRESS MSP Corporation 1313 Fifth St. SE Minneapolis, MN 55414	10. PROGRAM ELEMENT NO. A101/B/67/01-8048 11. CONTRACT/GRANT NO. P.O. No. 8D1432YASA
12. SPONSORING AGENCY NAME AND ADDRESS Atmospheric Research and Exposure Assessment Lab. Office of Research and Development U.S. Environmental Protection Agency Research Triangle Park, North Carolina 27711	13. TYPE OF REPORT AND PERIOD COVERED Final (2/88-5/89) 14. SPONSORING AGENCY CODE EPA/600/09

15. SUPPLEMENTARY NOTES
to be submitted for publication in Environmental Science and Technology

16. ABSTRACT

A compact coiled denuder has been designed and its performance evaluated both theoretically and experimentally. The design is based on special features of laminar flow in a curved tube, which significantly enhance the mass transfer Sherwood number governing gas collection at the wall. At 10 slpm the gas collection efficiency for SO_2, using a sodium carbonate/glycerine wall coating exceeds 99% and thus is comparable with annular denuder efficiencies. Measured losses for particles in the range of 0.02 to 2.5 um diameter averaged well under 5%. The short axial length (6 cm) of the coiled denuder has the advantage that a denuder train of multiple units in series will have a total length which is substantially less than a corresponding train of annular denuders.

17. KEY WORDS AND DOCUMENT ANALYSIS

a. DESCRIPTORS	b. IDENTIFIERS/OPEN ENDED TERMS	c. COSATI Field/Group

REPRODUCED BY
U.S. DEPARTMENT OF COMMERCE
NATIONAL TECHNICAL INFORMATION SERVICE
SPRINGFIELD, VA. 22161

18. DISTRIBUTION STATEMENT	19. SECURITY CLASS *(This Report)*	21. NO. OF PAGES
RELEASE TO PUBLIC	UNCLASSIFIED	7
	20. SECURITY CLASS *(This page)*	22. PRICE
	UNCLASSIFED	A02

EPA/600/J-90/030

Reprinted from ENVIRONMENTAL SCIENCE & TECHNOLOGY, Vol. 24, Page 307, March 1990
Copyright © 1990 by the American Chemical Society and reprinted by permission of the copyright owner.

NTIS is authorized to reproduce and sell this report. Permission for further reproduction must be obtained from the copyright owner.

A Compact Coiled Denuder for Atmospheric Sampling†

David Y. H. Pui,*,‡ Charles W. Lewis,§ Chuen-Jinn Tsai,‡ and Benjamin Y. H. Liu‡

Particle Technology Laboratory, Mechanical Engineering Department, University of Minnesota, 111 Church Street S. E., Minneapolis, Minnesota 55455, and U.S. Environmental Protection Agency, Atmospheric Research and Exposure Assessment Laboratory, Research Triangle Park, North Carolina 27711

■ A compact coiled denuder has been designed and its performance evaluated both theoretically and experimentally. The design is based on special features of laminar flow in a curved tube, which significantly enhance the mass-transfer Sherwood number governing gas collection at the wall. At 10 standard L/min (slpm) the gas collection efficiency for SO_2, using a sodium carbonate/glycerine wall coating, was measured to be 99.3 ± 0.5%, while losses for particles in the range of 0.02–2.5-μm diameter averaged well under 5%.

Introduction

Diffusion denuders have become increasingly popular for separating reactive gases from particles as a means to measuring their separate concentrations (*1–5*). The ideal denuder is a channel whose inner wall is a sink for a gas and is operated so that the trace reactive gas is collected with 100% efficiency on the wall while 100% of the particles traverse the channel, thus being available for collection on a downstream substrate in an airstream free of the reactive gas. If the gaseous sink is a reactive coating, the gas concentration can be determined by extracting the coating and measuring the amount of chemically transformed gas it contains. Denuders have proved to be particularly valuable in nitrogenous atmospheric chemistry, enabling accurate and artifact-free measurements of particulate nitrate and gaseous nitric and nitrous acids to be made simultaneously (*6*).

The invention of the annular denuder (*7*) significantly increased the practicality of denuders by reducing the required channel length to approximately 20 cm, about an order of magnitude less than that needed for a hollow straight tube denuder. However, since an annular denuder system may use as many as four such units (with coatings for different gases) in series along a common axis, the dimensions of the overall system can be inconvenient. Hence an even more compact denuder design would be desirable.

The denuder design examined in this article is a 1 cm i.d. glass tube bent into a three-turn, 10 cm diameter helical coil, intended to operate at 10 standard L/min (slpm). In the following sections the theoretical and experimental aspects of gas collection efficiency and particle transmission for this design will be presented.

Table I. Heat- and Mass-Transfer Correspondences

heat transfer	P_r	N_u	T	$\dot{q}$
mass transfer	S_c	S_h	C	$\dot{m}$

Theoretical Considerations

Heat- and Mass-Transfer Analogy. Because of the analogy between heat and mass transfer, researchers in these fields have often calculated the rate of heat transfer from mass-transfer data and vice versa. The corresponding parameters that are used in heat- and mass-transfer analogy are listed in Table I.

In Table I, P_r is the Prandtl number, which is defined as ν/α with ν the kinematic viscosity and α the thermal diffusivity; S_c is the Schmidt number, which is defined as ν/D with D the mass diffusivity; N_u is the Nusselt number, which is defined as $h(2a)/\kappa$ with h the heat-transfer coefficient, a the tube radius, and κ the thermal conductivity; S_h is the Sherwood number, which is defined as $k(2a)/D$ with k the mass-transfer coefficient; T is temperature; C is mass concentration; $\dot{q}$ is heat-transfer rate; $\dot{m}$ is mass-transfer rate. In the following analysis, heat-transfer relationships that will be used in the gas collection efficiency calculations are written in the corresponding mass-transfer forms.

Gas Collection Efficiency. The present coiled denuder design is based on the special features of laminar flow in curved pipes. This flow is characterized by secondary flow in any cross-sectional plane normal to the main flow, and an axial velocity profile that is skewed to the outer wall of the pipe due to centrifugal force. Figure 1 shows the secondary flow streamlines for a curved pipe, where the counterrotating vortexes continuously bring fluid in the interior near the pipe wall, with the result that mass-(and heat-)transfer efficiencies are significantly increased relative to the straight pipe case.

The nature of this flow depends on the Dean number D_e and curvature ratio R_o. Curvature ratio R_o is defined as R/a with R the radius of the coil and a the radius of the tube. The Dean number is defined as $D_e = R_e/\sqrt{R_o}$ with R_e the flow Reynolds number. The heat-transfer problem for fully developed flow in curved pipes has been solved analytically (*8–11*). Numerical studies of flow and heat transfer in curved pipes have been conducted (*12–15*). The heat-transfer analysis by Mori and Nakayama et al. (*8–10*) was based on the assumption that the flow can be

† Particle Technology Laboratory Publication no. 679.
‡ University of Minnesota.
§ U.S. Environmental Protection Agency.

0013-936X/90/0924-0307$02.50/0 © 1990 American Chemical Society

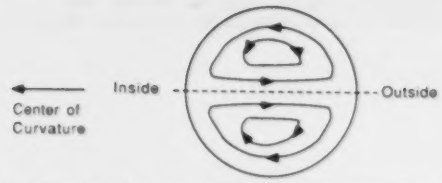

Figure 1. Secondary flow streamlines in the cross-sectional plane of the curved tubes. The axial velocity profile is skewed toward the outside of the tube.

divided into a core region and a boundary layer. This theoretical model was validated by the authors themselves (*8*) and consequently was considered to be the most rigorous for use in the present work.

Although turbulent flow is associated with a larger mass-transfer Sherwood number than laminar flow, larger inertial impaction loss of particles is, unfortunately, also likely with the former. Therefore in the current coiled denuder design, the flow is restricted to the laminar regime.

In a straight pipe, assuming the flow is fully developed and the concentration profile is developing, the mass-transfer efficiency, η (=1 − P, P is penetration), can be calculated as (from eq 8-31 in ref 16)

$$\eta = 1 - P \tag{1a}$$

$$P = \frac{C_{out}}{C_{in}} = \exp\left(-\frac{\pi L D}{Q}\bar{S}_h\right) \tag{1b}$$

where C_{in} is the inlet concentration, C_{out} is the outlet concentration, L is the pipe length, D is the gas diffusivity, Q is the flow rate, and $\bar{S}_h$ is the mean mass-transfer Sherwood number over the pipe length, equal to 3.66 for a fully developed temperature profile with constant wall temperature condition. In a curved pipe, following the suggestion made by Mori and Nakayama (*9*, *10*), the mass-transfer efficiency can also be calculated by using eq 1 if the mean mass-transfer Sherwood number is known.

In the laminar flow regime, Mori and Nakayama (*9*, *10*) showed that for fully developed flow (both velocity and concentration profiles), the mean mass-transfer Sherwood number, $\bar{S}_h$, in a curved pipe can be approximated as

$$\bar{S}_h = \frac{0.864}{\zeta} D_e^{1/2}(1 + 2.35 D_e^{-1/2}) \tag{2}$$

where

$$\zeta = \frac{2}{11}\left[1 + \left(1 + \frac{77}{4}\frac{1}{S_c^2}\right)^{1/2}\right] \quad \text{if } \zeta \le 1 \text{ (or } S_c \ge 1) \tag{3}$$

or

$$\zeta = \frac{1}{5}\left[2 + \left(\frac{10}{S_c^2} - 1\right)^{1/2}\right] \text{ if } \zeta \ge 1 \text{ (or } S_c \le 1) \tag{4}$$

where ζ is the thickness ratio of the concentration boundary layer to the momentum boundary layer.

Equation 2 is based on the assumption of a fully developed concentration boundary layer. At the point of entry, the Sherwood number has its maximum value since the concentration boundary layer is still developing. Figure 2 shows two best fit curves obtained from data of Sparrow and Chrysler (*17*). It shows the normalized Sherwood number S_h/S_h^* (S_h^* is the Sherwood number for a fully developed concentration profile) versus dimensionless tube length L/a at R_e = 5000 and 8200, when the flow can still be considered as laminar since both Reynolds numbers are

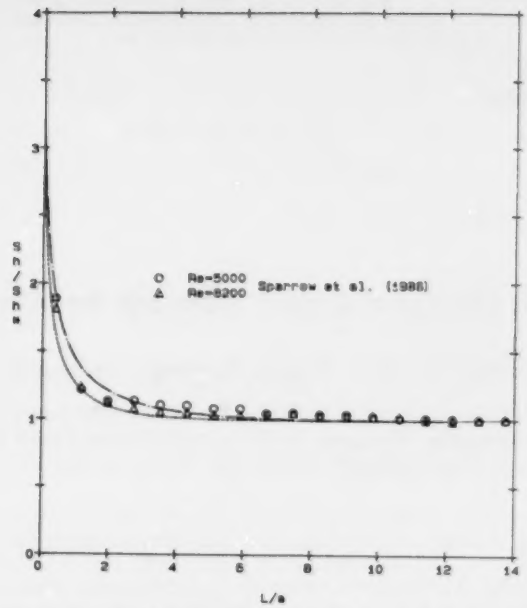

Figure 2. Normalized Sherwood number versus normalized tube length.

lower than the critical value 9900. [From Ito (*18*) the critical Reynolds number is $R_{e,cr} = 2 \times 10^4(R_o)^{-0.32} = 2 \times 10^4(9)^{-0.32} = 9900$. Ito's equation is valid for $R_o \le 860$; when $R_o > 860$, $R_{e,cr}$ approaches 2000–3000. Note that the present Reynolds number is 1407.] It is seen that the normalized Sherwood number quickly approaches unity monotonically as the concentration profile becomes fully developed. This Sherwood number length dependence is similar to the straight pipe case (*16*). The effect of the concentration entry length is to increase the overall mass-transfer efficiency or decrease penetration. To account for this entry length effect, a correction factor f_1, which is always smaller than 1.0, needs to be included in eq 1 as

$$P = \frac{C_{out}}{C_{in}} = f_1 \exp\left(-\frac{\pi L D}{Q}\bar{S}_h\right) \tag{5}$$

Because the dependence of Sherwood number on length is similar for curved and straight pipe flows, factor f_1 can be found by considering the entry length effect in a straight pipe flow, as follows.

In a straight pipe, assuming the flow is hydrodynamically fully developed and the concentration profile is still developing, the penetration can be calculated from the Gormley–Kennedy equation (*19*) as

$$P = 0.819\exp(-11.5\xi) + 0.0975\exp(-70.1\xi) + 0.0325\exp(-179\xi) \quad \text{for } \xi > 0.007 \tag{6}$$

where $\xi = DL/Q$. If ξ is large enough, only the first term in the right-hand side of the above equation is important. The coefficient 11.5 in the exponent is simply the product of π and $\bar{S}_h$, 3.66, which is the Sherwood number for fully developed flow in concentration, in the case of constant (zero) wall concentration. Comparing eq 5 and 6, it is seen that factor f_1 is 0.82 for large ξ. Alternatively, one can take the ratio of penetrations represented by eq 6 and 5 and plot the correction factor f_1 versus tube length as shown in Figure 3 assuming a = 0.5 cm, D = 0.136 cm^2/s, and three different flow rates of 5, 10, and 15 slpm. It is seen that factor f_1 approaches 0.82 when the tube length is greater than 30, 60, and 90 cm at flow rates of 5, 10, and 15 slpm, respectively. Therefore, in the present coiled

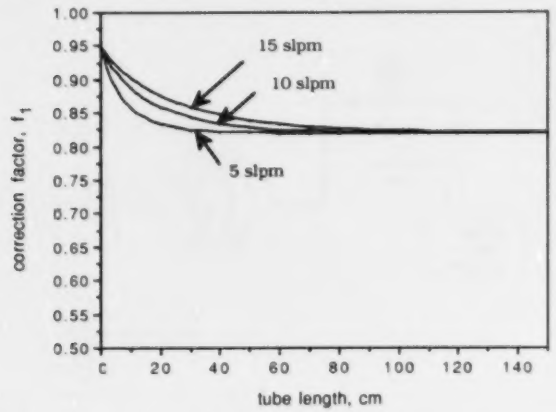

Figure 3. Correction factor f_1 versus tube length at different flow rates.

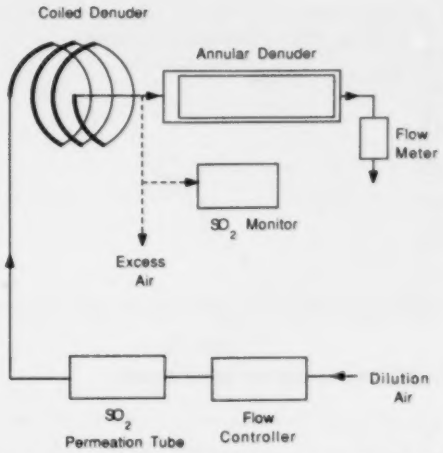

Figure 4. Experimental setup for measuring gas collection efficiency.

denuder design where the nominal flow rate is 10 slpm and the tube length is greater than 60 cm, the gas collection efficiency can be calculated as

$$\eta = 1 - P = 1 - 0.82 \exp\left(-\frac{\pi L D}{Q}\bar{S}_h\right) \qquad (7)$$

where the mean Sherwood number $\bar{S}_h$ can be calculated from eq 2. The present coiled denuder geometry gives a Sherwood number of 21.996, which is ~6 times that of straight pipe, 3.66. Hence, mass-transfer efficiency in coiled tubes is expected to be significantly larger than that in hollow straight tubes.

Particle Loss. Particle loss in any transport system can originate from many different mechanisms such as gravitational settling, diffusion, inertial impaction, and turbulent deposition. A concise review of various particle loss mechanisms in straight pipe flow can be found in ref 20. In a coiled tube, inertial impaction loss is important for particles greater than 1.0 μm in aerodynamic diameter, while diffusion loss is important for submicron particles. Experimental study for particle loss in a 90° bend by Pui et al. (*21*) indicated that inertial impaction loss is negligible when the particle Stokes number is smaller than 0.1. Using the numerical results obtained by Tsai et al. (*15*), an attempt was made to calculate the loss in one 90° bend and multiply it by 12 (the coiled denuder contains 12 90° bends) to obtain the total loss in the coiled denuder. However, since the flow inside the coiled denuder eventually becomes fully developed, the developing flow assumption in the numerical work resulted in an underestimation of inertial impaction loss as compared to the experimental results. On the other hand, a separate numerical study assuming a fully developed profile resulted in an overestimation of inertial impaction loss. This indicates that further numerical study of particle loss in coils would be desirable. For the purpose of the present study, an empirical fit to the inertial impaction loss, Loss_I, was used.

We were similarly unsuccessful in obtaining an analytical solution to diffusion loss, Loss_D, in a coiled denuder. Again, an empirical fit was used. Assuming both Loss_I and Loss_D are small, total particle loss in a coiled denuder can be written as

$$\begin{aligned}\text{loss (\%)} &= [1.0 - (1 - \text{Loss}_D)(1 - \text{Loss}_I)] \times 100 \\ &\approx [\text{Loss}_D + \text{Loss}_I] \times 100 \end{aligned} \qquad (8)$$

In the remainder of this article, we present the experimental characterization of the resulting coiled denuder design, which has achieved the design objectives of both high gas collection efficiency and low particle loss.

Experimental Methods and Results

Gas Collection Efficiency and Capacity. Gas collection efficiency measurements using SO_2 were performed with the experimental arrangement shown in Figure 4. The basis of the measurements was to determine the amounts of SO_2 simultaneously collected in the coiled denuder and in an efficient downstream collector, an annular denuder (University Research Glassware Co., Model 2000-30B). The efficiency can then be calculated from

$$\text{coil efficiency (\%)} = \frac{M_{\text{coil}}}{M_{\text{coil}} + M_{\text{annular}}} \times 100 \qquad (9)$$

where each M is the mass of SO_2 collected on the specified component.

For each measurement set the previously roughened (by sandblasting with no. 100 grain carborundum) interior wall of the coiled denuder was coated with a Na_2CO_3/glycerine solution in a methanol and distilled water mixture, in the manner previously described (*6*). The same coating was applied to the annular denuder. After exposure to the SO_2 gas stream both denuders were extracted (*6*) and the extracts were analyzed for both sulfite and sulfate by ion chromatography. Sulfur dioxide reacts with Na_2CO_3 to form sulfite, but since this gradually oxidizes to sulfate, the total amount of collected SO_2 must be inferred from the concentrations of both sulfur species. Sodium carbonate/glycerine coating solution concentrations of 1%/1%, the "standard" coating, and 5%/5% were both used in separate experiments. SO_2 breakthrough experiments were conducted for both coating solutions, using the alternative arrangement shown by dashed lines in Figure 4, to ensure that SO_2 sampling times for the efficiency measurements were shorter than the time for which coating depletion was first perceptible.

Figure 5 shows a typical breakthrough result. The TECO Model 43 pulsed fluorescence SO_2 analyzer used has a detection limit near 1 ppb, compared with the SO_2 test concentration of ~70 ppb. A breakthrough product of 700 ppb-h, or 1 mg of SO_2, can be inferred from Figure 5. It must be understood that this value is only a lower limit for the device's capacity under typical field conditions. This is because the laboratory measurements happened to be performed at extremely low relative humidity, estimated to be <10%. In general, the capacity of the coiled denuder should be similar to that of the previously mentioned annular denuder, since the wall areas of the two

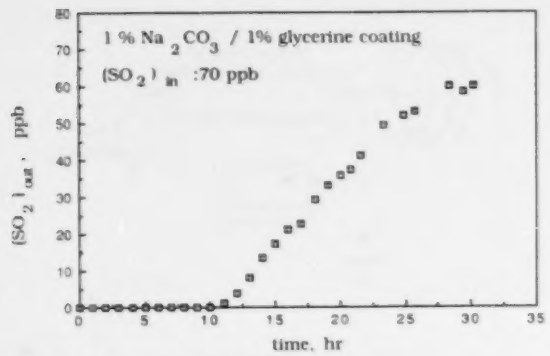

Figure 5. SO_2 breakthrough for coiled denuder.

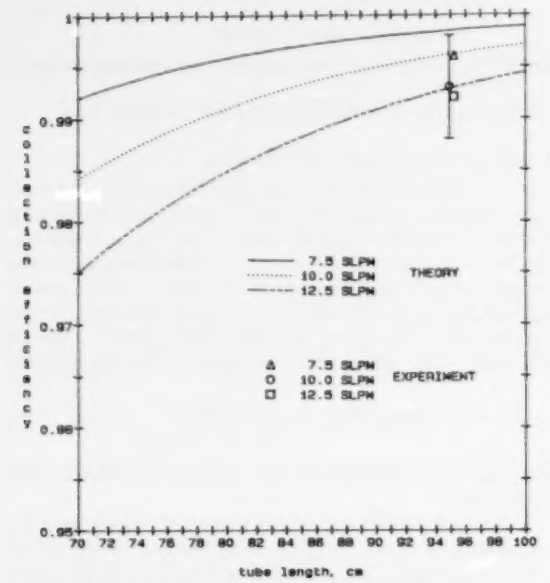

Figure 6. Coiled denuder gas collection efficiency versus tube length at different flow rates.

devices are nearly the same.

From a total of six determinations at 10 slpm the coiled denuder SO_2 gas collection efficiency was found to be 99.3 ± 0.5% (mean ± SD). One measurement each at 7.5 and 12.5 slpm gave efficiencies of 99.6 and 99.2%, respectively. The comparison of theory (eq 7) and experiment shown in Figure 6 indicates resonable agreement. Finally, three runs at 10 slpm were performed with the coiled denuder replaced by a second annular denuder. The annular denuder efficiency was found to be ≥99.9% in all cases, consistent with its use as an efficient downstream collector for the coiled denuder efficiency measurements.

Particle Loss. Particle loss measurement has been performed for particle sizes ranging from 0.015 to 5.4 μm. Results for monodisperse aerosol between 1.0 and 5.4 μm aerodynamic diameter were obtained with a vibrating orifice aerosol generator (TSI Model 3450) operated as part of the experimental system shown in Figure 7a. The monodispersity of the aerosol was monitored by an Aerodynamic Particle Sizer (APS, TSI Model 33). The liquid used in the aerosol generator consisted of oleic acid dissolved in denatured alcohol and containing a small quantity of uranine (1 g/L) as a fluorescent tracer. That is, the amounts of uranine measured on the coiled denuder and downstream filter are proportional to the amounts of particles deposited on these components. The solution

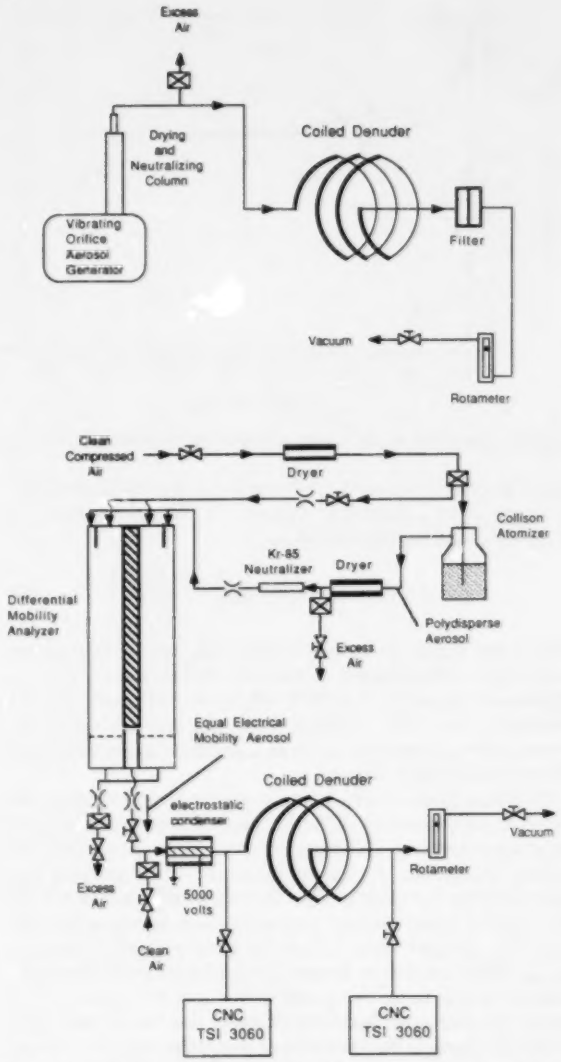

Figure 7. (a) Schematic diagram of particle loss test system, $D_p \geq 1.0$ μm. (b) Schematic diagram of particle loss test system, $D_p < 1.0$ μm. (neutral particles)

used to wash the filter and denuder was 15 or 30 mL of 0.001 N NaOH. The deposited particle mass is proportional to the product of the measured uranine concentration and the amount of washing solution used. The particle loss in the denuder was then calculated from

$$\text{loss (\%)} = \frac{M_{\text{coil}}}{M_{\text{coil}} + M_{\text{filter}}} \times 100 \qquad (10)$$

where M_{coil} and M_{filter} are the deposited particle masses in the coiled denuder and filter, respectively. Particle loss was determined at three different flow rates, 7.5, 10, and 12.5 slpm. The accuracy of the measurements was estimated to be ±1% for particles from 1 to 3 μm and ±3% for particles above 3 μm in aerodynamic diameter.

For submicron particles, the experimental system shown in Figure 7b was used. A Collison atomizer generated polydisperse aerosol by spraying NaCl solution of 0.05, 0.5, or 10% volume concentration. The particles were dried in a diffusion dryer and passed through a ^{85}Kr neutralizer. The polydisperse aerosol was then classified by a differential mobility classifier (DMA, TSI Model 3702). By varying the voltage supplied to the center rod inside the

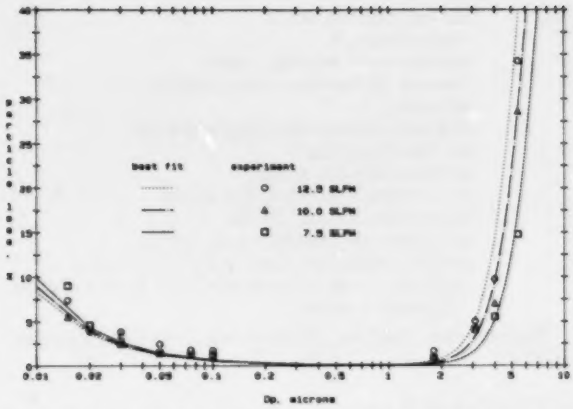

Figure 8. Total particle loss in coiled denuder at three different flow rates (neutral particles).

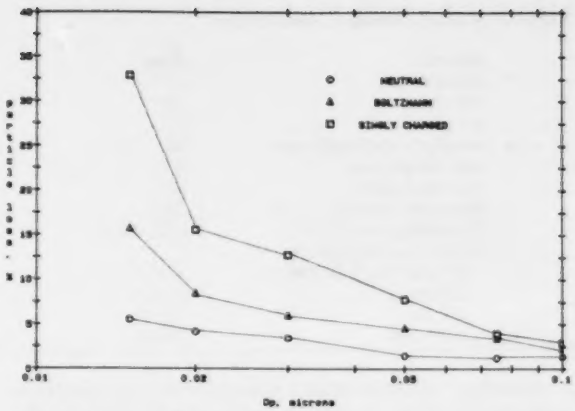

Figure 9. Effect of different charge states of test aerosol on particle loss, 10 slpm.

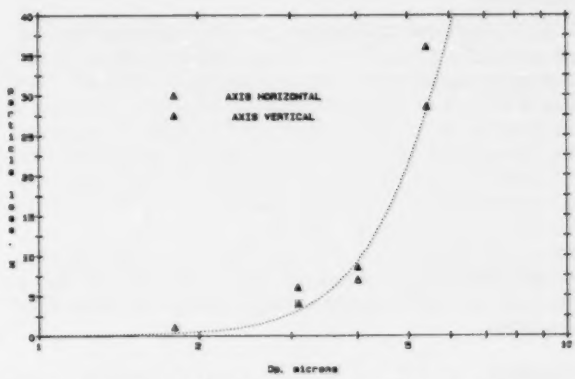

Figure 10. Effect of orientation on particle loss at 10 slpm.

DMA a monodisperse aerosol of equal electric mobility can be generated, as described by Liu and Pui (22). Most of the monodisperse submicron particles emerging from the DMA carry a single elementary charge. To obtain neutral particles for the experiment, this aerosol was passed through an electrostatic condenser to remove all charged particles. Two other tests were also conducted using Boltzmann equilibrium and singly charged aerosols to investigate the effect of electrical charge on particle loss. For the singly charged particle loss test, the aerosol coming out of the DMA was used directly. The Boltzmann equilibrium aerosol was obtained by neutralizing the aerosol before entering the coiled denuder. Downstream (C_{out}) and upstream (C_{in}) aerosol concentrations were measured by condensation nuclei counters (CNC, TSI Model 3060). Particle loss can then be computed as $1 - C_{out}/C_{in}$. The test was conducted at the same three previous flow rates. The accuracy of the particle loss results was estimated to be ±2% for particles greater than 0.02 μm and ±4% for particles less than 0.02 μm.

A fit to the experimental results for particles greater than 1 μm can be expressed in the following form:

$$\text{Loss}_I = 1/(1 + 0.0017(St_K)^{(-2.24)}) \qquad (11)$$

For diffusion loss of submicron particles the conventional Gormley–Kennedy equation for a straight tube was found to underestimate the experimental particle loss in the coiled denuder by a factor of 2–3. By use of a form similar to that for particle loss in straight tube, a fit to the experimental neutral particle loss data for particles smaller than 1 μm resulted in the following form:

$$\text{Loss}_D = 1.83\xi_1^{2/3} - 1.26\xi_1 \qquad (12)$$

where $\xi_1 = (\pi LD/11.5\,Q)\bar{S}_h$. Note for a straight tube, the coefficients of the first and second terms are 5.5 and 3.77, respectively, with ξ_1 replaced by LD/Q (eq 7.29 in ref 23).

Figure 8 shows the experimental total particle losses, including both the inertial impaction and diffusion losses, and those given by eq 8 at 7.5, 10, and 12.5 slpm. Note the diffusion losses refer to neutral particles. Since denuders are generally used with preclassifier inlets having cut points near 2.5 μm, the high losses measured above this particle size are unimportant. The submicron neutral particle loss is also small. At 0.015 μm, the loss is 6 ± 4%, and at 0.1 μm the loss is 2 ± 2%.

The results shown in Figure 8 apply for the test made with neutral particles in the submicron range. The effect of different charge states of test aerosol on submicron particle loss is shown in Figure 9. It is seen that the aerosol charge enhances the loss substantially. The neutral aerosol always has the smallest loss, with increasingly higher losses for Boltzmann equilibrium and singly charged states, respectively. For use of this apparatus in atmospheric sampling, the test results for the Boltzmann equilibrium case are the most relevant. The neutral particle losses were very reproducible, but the Boltzmann and singly charged tests showed considerably day to day variation. This is the reason for emphasizing the neutral particle results in this article. Charges in relative humidity were undoubtedly an important factor in this variation, but we have no comprehensive understanding of the effect.

While extremely low humidity will likely impair the device's operation, due to electrostatic and premature coating depletion effects, very high humidity may also be troublesome: the hygroscopicity of the glycerine in the coating may accumulate so much water that the coating may run off the denuder surfaces. Some control of this can be achieved by decreasing the glycerine content of the coating solution.

The effect of orientation on particle loss was also investigated and is shown in Figure 10 for particles larger than 1 μm. It is seen that the total particle loss is only slightly higher when the coiled denuder axis is vertical, compared to the horizontal case. Hence, it is concluded that the coiled denuder can be operated in any orientation.

The particle test data presented above apply to a smooth uncoated tube. Limited measurements have shown that results for an uncoated sand blasted tube are similar. Extensive measurements (24) comparing particle losses for coated versus uncoated *annular* denuders have shown smaller losses for the coated cases, presumably because of

Table II. Coiled Denuder Description

material	glass
tube i.d., cm	1
coil diam, cm	10
no. of turns	3
uncoiled tube length, cm	95
axial length, cm	6
flow rate, slpm	10
Reynolds number	1407
SO_2 collection effic, %	99.3 ± 0.5
neutral particle loss, %	
2.5 μm (St_k = 0.0086)	1 ± 1
1.0 μm	0 ± 1
0.1 μm	2 ± 2
0.015 μm	6 ± 4

a reduction of electrostatic effects from the electrical conductivity of the coating. It can be anticipated that the same will hold for the coiled denuder.

Summary

A 10 slpm coiled denuder has been designed and experimentally characterized. Its geometrical parameters and operating characteristics are summarized in Table II. The gas collection efficiency for SO_2 exceeds 99% and thus is comparable with annular denuder efficiencies. Experiment has shown that the particle loss is small for neutral particles in the size range 0.015–2.5 μm. Particle loss measurements also indicate that the unit can operate equally well in any orientation. The short axial length (6 cm) of the coiled denuder has the advantage that a denuder train of multiple units in series will have a total length that is substantially less than a corresponding train of annular denuders.

Glossary

a	tube radius, cm
C	mass (particle) concentration, g/cm³ (no./cm³) C_{out}, outlet concentration; C_{in} inlet concentration
C_c	slip correction factor
c	specific heat at constant pressure, erg/(g K)
D	mass diffusivity, cm²/s
D_e	Dean number, $R_e/\sqrt{R_o}$
D_p	particle diameter, cm
f_1	correction factor
h	heat-transfer coefficient, erg/(s cm² K)
k	mass-transfer coefficient, cm/s
L	tube length, cm
loss	particle loss $Loss_I$, inertial impaction loss in coiled denuder, decimal value $Loss_D$, diffusion loss in coiled denuder, decimal value loss (%), total particle loss, %
M	particle (or SO_2) mass M_{coil}, mass collected in coiled denuder M_{filter}, mass collected in filter $M_{annular}$, mass collected in annular denuder
$\dot{m}$	mass (particle) transfer rate, g/s (no./s)
N_u	Nusselt number, $h(2a)/\kappa$
P	penetration, C_{out}/C_{in}
P_r	Prandtl number, ν/α
Q	volumetric flow rate, cm³/s
$\dot{q}$	heat-transfer rate, erg/s
R	coil radius, cm
R_e	Reynolds number, $\rho\bar{w}(2a)/\mu$
R_o	curvature ratio, R/a
S_c	Schmidt number, ν/D
S_h	Sherwood number, $k(2a)/D$
$\bar{S}_h$	mean Sherwood number
S_h^*	fully developed Sherwood number
St_k	Stokes number, $\bar{w}\tau/a$
T	temperature, K
$\bar{w}$	average axial velocity, cm/s
α	thermal diffusivity, $\kappa/(\rho c)$, cm²/s
η	efficiency, 1 − P
κ	thermal conductivity, erg/(s cm K)
ρ	air density, g/cm³
ρ_p	particle density, g/cm³
μ	air dynamic viscosity, dyn s/cm²
ξ	parameter in eq 6, DL/Q
ν	air kinematic viscosity, μ/ρ, cm²/s
τ	particle relaxation time, $\rho_p D_p^2 C_c/(18\ \mu)$, s
ζ	thickness ratio of concentration to momentum boundary layer

Registry No. Na_2CO_3, 497-19-8; SO_2, 7446-09-5; glycerine, 56-81-5.

Literature Cited

(1) Stevens, R. K.; Dzubay, T. G.; Russwurm, G.; Rickel, D. *Atmos. Environ.* **1978**, *12*, 55.
(2) Forrest, J.; Spandau, D. J.; Tanner, R. L.; Newman, L. *Atmos. Environ.* **1982**, *16*, 1473.
(3) Braman, R. S.; Shelley, T. J.; McClenny, W. A. *Anal. Chem.* **1982**, *54*, 358.
(4) Ferm, M.; Sjödin A. *Atmos. Environ.* **1985**, *19*, 985.
(5) Durham, J. L.; Spiller, L. L.; Ellestad, T. G. *Atmos. Environ.* **1987**, *21*, 589.
(6) Vossler, T. L.; Stevens, R. K.; Paur, R. J.; Baumgardner, R. E.; Bell, J. P. *Atmos. Environ.* **1988**, *22*, 1729.
(7) Possanzini, M.; Febo, A.; Liberti, A. *Atmos. Environ.* **1983**, *17*, 2605.
(8) Mori, Y.; Nakayama, W. *Int. J. Heat Mass Transfer* **1965**, *8*, 67.
(9) Mori, Y.; Nakayama, W. *Int. J. Heat Mass Transfer* **1967**, *10*, 37.
(10) Mori, Y.; Nakayama, W. *Int. J. Heat Mass Transfer* **1967**, *10*, 681.
(11) McConalogue, D. J.; Srivastava, R. S. *Proc. R. Soc. London, A* **1968**, *307*, 37.
(12) Patankar, S. V.; Pratap, V. S.; Spalding, D. B. *J. Fluid Mech.* **1974**, *62*, 539.
(13) Soh, W. Y.; Berger, S. A. *J. Fluid Mech.* **1984**, *148*, 109.
(14) Humphrey, J. A. C.; Iacovides, H.; Launder, B. E. *J. Fluid Mech.* **1985**, *154*, 357.
(15) Tsai, C. J.; Pui, D. Y. H. *Aerosol Sci. Technol.*, in press.
(16) Kays, W. M.; Crawford, M. E. *Convective Heat and Mass Transfer*, 2nd ed.; McGraw-Hill Book Co.: New York, 1980.
(17) Sparrow, E. M.; Chrysler, G. M. *J. Heat Transfer* **1986**, *108*, 40.
(18) Ito, H. *J. Basic Eng.* **1959**, *81D*, 123.
(19) Gormley, P.; Kennedy, M. *Proc. R. Ir. Acad.* **1949**, *52A*, 163.
(20) Liu, B. Y. H.; Pui, D. Y. H.; Rubow, K. L.; Szymanski, W. W. *Ann. Occup. Hyg.* **1985**, *29*, 251.
(21) Pui, D. Y. H.; Romay-Novas, F.; Liu, B. Y. H. *Aerosol Sci. Technol.* **1987**, *7*, 301.
(22) Liu, B. Y. H.; Pui, D. Y. H. *J. Colloid Interface Sci.* **1974**, *47*, 155.
(23) Hinds, W. C. *Aerosol Technology*; John Wiley & Sons: New York, 1982.
(24) Ye, Y.; Tsai, C.-J.; Pui, D. Y. H.; Lewis, C. W. Presented at AAAR 1989 Annual Meeting, Reno, NV; submitted for publication in *Aerosol Sci. Technol.*

Received for review May 11, 1989. Accepted October 24, 1989. This work was supported by the U.S. Environmental Protection Agency under Purchase Order No. 8D1432YASA. Although the research described in this article has been funded by the U.S. EPA, it has not been subjected to Agency review and, therefore, does not necessarily reflect the views of the Agency, and no official endorsement should be inferred. Mention of commercial products does not constitute endorsement by U.S. EPA. We thank Suzanna Browne, John Bell, and Bill Karches for their help in performing the gas collection efficiency measurements.